Journal of
Experimental & Applied Mechanics
https://journals.stmjournals.com/joeam

ISSN: 2230-9845 (Online)
ISSN: 2321-516X (Print)
Volume 15, Issue 3, 2024
September–December
DOI (Journal): 10.37591/JoEAM

Research JoEAM

Effects of Bearing Design Parameter on Working Characteristics of Floating Ring Bearing

Son Gun Kwon[1], Chol Min Ri[2], Sol Song Pak[3,*]

Abstract

The working stability of turbochargers supported by floating ring bearings depends on not only the structure of the rotors but also working characteristic of floating ring bearings. These working characteristics are related to working conditions and design parameters of floating ring bearings. The main goal of this research is to investigate the working characteristics of bearings by design parameters of floating ring bearings. In order to study the working characteristics of bearings, turbocharger supported in FRBs are modeled as multi-body systems and the inner characteristics of FLBs are described by the Reynold's equation. Numerical analysis about the interaction of the rotor-FRB system is taken by using time integral method and calculus of finite differences. Analysis of the influence of design parameter is taken in the main working field. Through this analysis, we can know that the tolerance ratio is the main factor in the floating ring bearing any other than the diameter ratio and length ratio and more convenient to regulate. It is more helpful to improve the dynamical response of turbocharger that we analysis the influence of design parameters of FRBs on the working characteristics of bearings.

Keywords: Rotordynamics, turbocharger, journal bearing, floating ring bearing

INTRODUCTION

Floating ring bearings(FRBs) are the most common type used for commercial turbocharger to minimize cost and power loss.

It is important to investigate the dynamics of high-speed turbocharger to control its vibration and guarantee safe operation.

It is very important to investigate the dynamics of bearings in improving the vibration characteristics of turbochargers and guaranting the stable working conditions.

Turbocharger supported in FRBs often operates at high speed under high temperature condition.

The coupling of excessive oil self-excited vibration and unbalance forced response will generate the turbocharger dissonant noise, seriously result in turbine or the compressor impeller wear and then cause the rotor-bearing system failure, thus reduce the operation efficiency and the life of turbocharger.

Generally, the modelling consists of two main stages. The equations of motion of a standalone rotor should be created on one hand and the problem of forces transmitted by floating ring bearings on the other hand.

Lumped parameter models [1–3] and nowadays more finite element models [4–6] are employed for the rotor modelling.

*Author For Correspondence
Sol Song Pak
E-mail: ss.pak@star-co.net.kp

[1-3]Faculty of Dynamics, Kim Il Sung University, Taesong District, Pyongyang, DPR Korea

Received Date: July 12, 2024
Accepted Date: October 28 , 2024
Published Date: December 11, 2024

Citation: Son Gun Kwon, Chol Min Ri, Sol Song Pak. Effects of Bearing Design Parameter on Working Characteristics of Floating Ring Bearing. Journal of Experimental & Applied Mechanics. 2024; 15(3):39–52p.

Considering the rotor gyroscopic moments and shaft flexibility, LI, et al, presented a lumped parameter model to numerically investigate the self-excited response of a high-speed turbocharger rotor-FRB system and the nonlinear characteristics of limit cycles was obtained, which provided new theory standards for the design of the FRBs. Generally floating ring bearings have two strong bearing clearance, geometric ratios, that is, inner and outer length, external clearance, inner and outer diameter of FRBs [4].

These six amounts are affected to the dynamic characteristics of rotor-floating ring bearing system.

The influence of the outer tolerance was investigated in [6] and [7] presented the method to decide the tolerance of FRBs on the basis of the measured response.

[9] Investigated the influence of the unbalanced vibration on different working conditions in the supply pressure and temperature of oil [10].

KIRK, et al, predicted the stability and transient dynamics phenomenon of the rotor system for turbocharger, which found that the oil whirl frequency spectrum are similar to the experimental results.

[11] shows the relation between the rotating velocity and minimum tolerance of bearings.

TIAN, et al [12], discussed the effect of bearing outer clearance on the rotor dynamic characteristics by using the run-up and run-down simulation method.

SHI, et al [13], studied the effects of clearance ratio of the inner to outer oil film in FRBs on turbocharger rotor instability.

The results show that when clearance ratio is small, the inner oil whirl dominates the instability regions of the rotor system [14,15].

ZHAO, et al [16], presented the FE model of rotor-bearing system by using the software DyRoBeS and analyzed dynamical characteristics in different working conditions of bearing such as span, width, gap and so on.

The results show that influence of parameters on the system dynamic characteristics is different.

As you can see in real tests and investigations, the influences of inner and outer tolerance of FRBs are big deal.

The variety of inner and outer tolerance is very important in working characteristics of FRBs and it may spoil the inherent characters of FRBs.

The main parameters are inner and outer length, inner and outer tolerance and inner and outer diameter in the FRBs.

But investigations about the working characteristics of FRBs are not so much.

This paper analyzed the influence of main design parameters on working characteristics of FRBs and found the good design parameters and its field.

This investigation is helpful to control the combination of FRB tolerance clearance for high-speed turbocharger.

SIMULATION MODEL OF TURBOCHARGER AND RESEARCH

The main task of research is to analyze working characteristics of floating bearing in total working velocity range of turbocharger.

Journal of Experimental & Applied Mechanics
Volume 15, Issue 3
ISSN: 2230-9845 (Online), ISSN: 2321-516X (Print)

As shown in Figure 1, this system consists of a rotating shaft and a floating ring bearing.

Turbine wheels and compressor wheels can be seen as rigid bodies [17].

However, the flow ring is realized as a rigid body using the MBS method with 2-5 degrees of freedom.

The housing is assumed to be fixed, and is therefore identical to the inertial frame for simplicity.

The support is modeled by the force and moment resulting from the kinematic state between the body by a nonlinear force law based on the hydrodynamic equations acting between the shaft, the flow ring and the body.

The rotor system is excited by external loads due to the imbalance of compressor and turbine wheel.

In addition, gravity is taken into account because it is the only directional force that results in a static part of the bearing load, which extends the rotor stability.

The Multibody System (MBS) method is widely used to simulate turbine turbocharger-rotor dynamics.

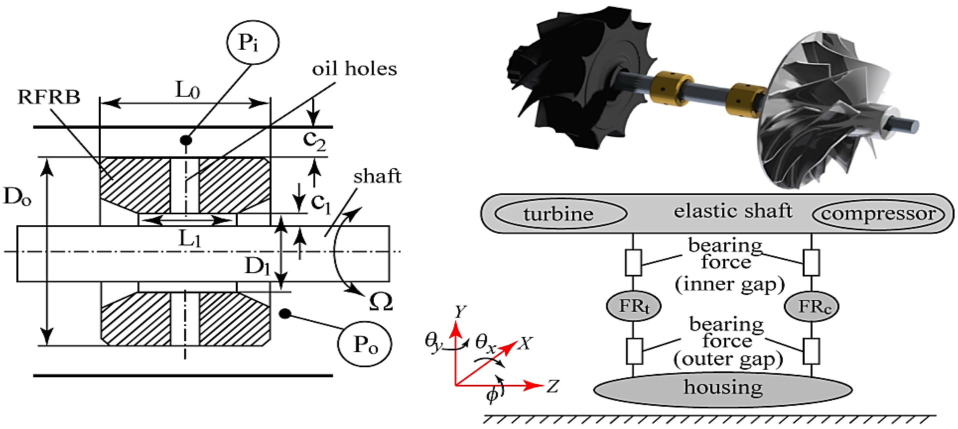

Figure 1. CAD of turbocharger.

The parameters of the turbochargers are given Table 1.

Table 1. simulation parameters.

Simulation parameter	**Unit**	**Value**
Mass of turbine blade	kg	0.556
Product inertia moment of TB	$kgmm^2$	178.4
Polar inertia moment of TB	$kgmm^2$	203.8
Mass of compressor blade	kg	0.158
Product inertia moment of CB	$kgmm^2$	61.24
Polar inertia moment of CB	$kgmm^2$	92.54
Mass of ring	kg	0.027
Outer diameter of ring	mm	22.1
Inner diameter of ring	mm	14.5
Outer radial clearance of bearing	μm	40.5
Inner radial clearance of bearing	μm	18.5
Inner length of bearing	mm	8.5
Outer length of bearing	mm	10.2
Length of turbocharger rotor	mm	236 SAE 15W-40
Supply pressure of oil	Mpa	0.3

Figure 2 shows the boundary conditions in inner and outer oil film of floating bearing.

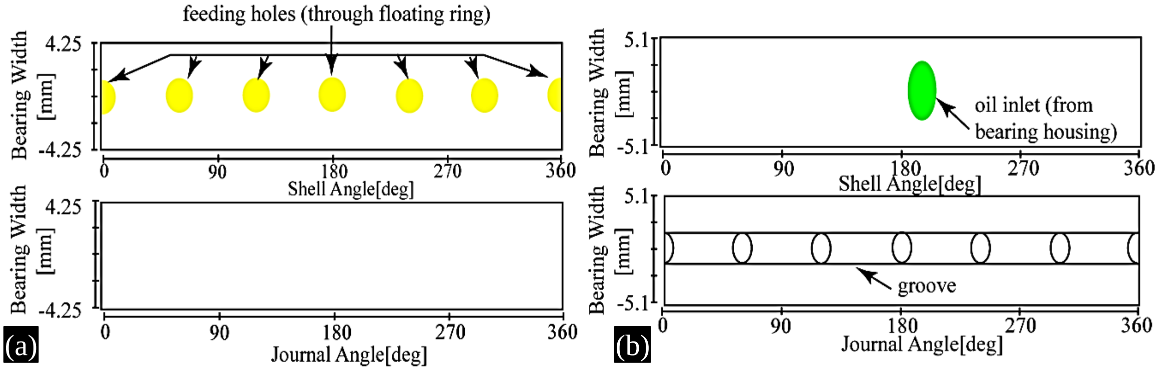

Figure 2. Boundary conditions of inner film (a) and outer film (b).

MATHEMATICAL MODELING

Turbocharger as a multi-body system

The rotor of the turbocharger supported in FRBs showed in Figure 1 is modeled as the FE model.

The motion equation for the turbocharger rotor system is expressed as:

$$[M_R]\{\ddot{U}_R\} + [C_R + G_R]\{\dot{U}_R\} + [K_R]\{U_R\} = -\{W_R\} + \{F_u\} + \{Fh_{inner}\} \tag{1}$$

Where $[M_R]$ is the mass matrix of the ring, $[C_R]$ is the damping matrix of rotor, $[G_R]$ is the gyroscopic matrix and $[K_R]$ is the stiffness matrix of rotor.

$$\{U_R\} = \{X_1, \theta_{Y1}, X_2, \theta_{Y2}, \dots, X_n, \theta_{Yn}, Y_1, \theta_{X1}, Y_2, \theta_{X2}, \dots, Y_n, \theta_{Xn}\}$$

$$\{U_R\} = \{X_1, \theta_{Y1}, X_2, \theta_{Y2}, \dots, X_n, \theta_{Yn}, Y_1, \theta_{X1}, Y_2, \theta_{X2}, \dots, Y_n, \theta_{Xn}\}$$

Therefore, the motion equation for the ring is given by:

$$[M_r]\{\ddot{U}_r\} = \{Fh_{outer}\} - \{Fh_{inner}\} - \{W_r\} + \{P_{in}\} \tag{2}$$

Where $\{U_r\}$ represents the displacement vector of the ring, and $[M_r]$ is the mass matrix of the ring.

The exciting force vectors include hydrodynamic forces of the two oil films, the lubricant feed pressure and the dead weight.

The motion equation for the turbocharger rotor system is then expressed in Equation.

$$\begin{bmatrix}[M_R] & [0]\\ [0] & [M_r]\end{bmatrix}\begin{Bmatrix}\ddot{U}_R\\ \ddot{U}_r\end{Bmatrix} + \begin{bmatrix}[C_R + G_R] & [0]\\ [0] & [0]\end{bmatrix}\begin{Bmatrix}\dot{U}_R\\ \dot{U}_r\end{Bmatrix} + \begin{bmatrix}[K_R] & [0]\\ [0] & [0]\end{bmatrix}\begin{Bmatrix}U_R\\ U_r\end{Bmatrix} = \tag{3}$$

$$= \begin{Bmatrix}F_u\\ 0\end{Bmatrix} - \begin{Bmatrix}W_R\\ W_r\end{Bmatrix} - \begin{Bmatrix}0\\ P_{in}\end{Bmatrix} + \begin{Bmatrix}Fh_{inner}\\ Fh_{outer} - Fh_{inner}\end{Bmatrix}$$

simplified

$$[M]\{\ddot{q}\} + [D]\{\dot{q}\} + [K]\{q\} = \{F^a\} + \{F^{oil}\} \tag{4}$$

where

$$[M] = \begin{bmatrix}[M_R] & [0]\\ [0] & [M_r]\end{bmatrix}, [D] = \begin{bmatrix}[C_R + G_R] & [0]\\ [0] & [0]\end{bmatrix}, [K] = \begin{bmatrix}[K_R] & [0]\\ [0] & [0]\end{bmatrix}$$

$$\{F^a\} = \begin{Bmatrix}F_u\\ 0\end{Bmatrix} - \begin{Bmatrix}W_R\\ W_r\end{Bmatrix} - \begin{Bmatrix}0\\ P_{in}\end{Bmatrix}, \{F^{oil}\} = \begin{Bmatrix}Fh_{inner}\\ Fh_{outer} - Fh_{inner}\end{Bmatrix}$$

Solving method of equation (4) was described in [23].

Hydrodynamic Bearings

As shown in Figure 2, the working principle of radial bearing is based on the hydrodynamic effect described by the Reynolds lubrication equation.

The pressure of the oil film is induced by the wedge contour between the bearing and journal whose velocities are Ω_r and Ω_j , respectively.

Lubricating oil is squeezed in the converged wedge by the rotation of the journal and bearing. Therefore, the oil pressure increases and reaches the maximum pressure.

The induced pressure of the oil film in the converged wedge generates the bearing forces acting upon the journal to keep the rotor stable in the radial direction [18].

The fluid dynamical pressure field can be calculated by the repaired Reynolds equation given by the Navier-Stocks equation and continuum equation, when the following assumptions are used.

The suggested approach for journal bearing model assumes generally known simplification assumptions, thin film theory assumptions, such states presents for example Hori [13].

In general, the ratio of the thickness to radius varies between 102 and 103 for the journal bearings considered allowing all second order terms to be neglected for a solution.

The mass in oil film can be negligible and the pressure is assumed to be constant in the thickness direction of oil film [19].

All external forces are negligible and there is no slip of the fluid at the walls.

Attention is required to define the dynamic viscosity of the lubricant.

The lubricant flow in the journal plain bearing can be described according to the simplified form of the Reynolds equation as follows :

$$\frac{\partial}{\partial x}\left(\frac{h^3}{12\eta}\frac{\partial p}{\partial x}\right)+\frac{\partial}{\partial z}\left(\frac{h^3}{12\eta}\frac{\partial p}{\partial z}\right)=\frac{u_j-u_b}{2}\frac{\partial h}{\partial x}+\frac{\partial h}{\partial t} \tag{5}$$

where x and z are coordinates of a point in lubricating film, t is time.

Figure 3 shows the cross section at the middle plane of one of the two identical FRBs.

The fixed reference frame ObXYZ is in agreement with the inertia frame given in Figure 1, where Ob denotes the bearing origin.

The ObZ axis cannot be shown as it is perpendicular to the depicted plane.

The Reynolds equations can be written like this.

$$\frac{1}{\mathrm{R}_j^2}\frac{\partial}{\partial\theta_i}\left[\frac{h_i^3}{12\eta_i}\frac{\partial p_i}{\partial\theta_i}\right]+\frac{\partial}{\partial z_i}\left[\frac{h_i^3}{12\eta_i}\frac{\partial p_i}{\partial z_i}\right]=\frac{\Omega_j+\Omega_r}{2}\frac{\partial h_i}{\partial\theta_i}+\frac{\partial h_i}{\partial t} \tag{6}$$

$$\frac{1}{\mathrm{R}_{ro}^2}\frac{\partial}{\partial\theta_o}\left[\frac{h_o^3}{12\eta_o}\frac{\partial p_o}{\partial\theta_o}\right]+\frac{\partial}{\partial z_o}\left[\frac{h_o^3}{12\eta_o}\frac{\partial p_o}{\partial z_o}\right]=\frac{\Omega_r}{2}\frac{\partial h_o}{\partial\theta_o}+\frac{\partial h_o}{\partial t} \tag{7}$$

where subscripts i and o identify the parameters of the inner oil film and outer oil film, Rj and Rro correspond to the journal radius and floating ring outer radius,. θ is the angular coordinate for the inner and outer oil films corresponding to the fixed frame, Zi and Zo are the axial coordinates of the inner and outer films, respectively

Boundary conditions are as follows.

$$p_i = \begin{cases} 0 & A \in \{A_{sid}\}, \\ p_{in} & A \in \{A_{in}\}, \end{cases} \tag{8}$$

$$p_o = \begin{cases} 0 & A \in \{A_{sid}\} \\ p_b & A \in \{A_{in}\} \\ p_{in} & A \in \{A_{out}\} \end{cases} \tag{9}$$

where p_{in} is inlet lubricant pressure, p_b is lubricant pressure of inner and outer oil film, A_{in} is a lubricant inlet area, A_{out} is a lubricant outlet area, A_{sid} is an area of lubricant side outlet and A is area [20].

The oil film thickness $h_i h_o$, $\frac{\partial h_i}{\partial t}$ and $\frac{\partial h_o}{\partial t}$ can be expressed by coordinates as follows:

$$h_i(\theta_i, \text{t}) = c_i - x_j cos\theta_i - y_j sin\theta_i \tag{10}$$

$$h_o(\theta_o, \text{t}) = c_o - X_r cos\theta_o - Y_r sin\theta_o \tag{11}$$

$$\frac{\partial h_i}{\partial t} = -(\dot{x}_j cos\theta_i + \dot{y}_j sin\theta_i) \tag{12}$$

$$\frac{\partial h_o}{\partial t} = -(\dot{X}_r cos\theta_o + \dot{Y}_r sin\theta_o) \tag{13}$$

$$\begin{cases} x_j = X_j - X_r \\ y_j = Y_j - Y_r \end{cases} \tag{14}$$

$$\begin{cases} \dot{x}_j = \dot{X}_j - \dot{X}_r \\ \dot{y}_j = \dot{Y}_j - \dot{Y}_r \end{cases} \tag{15}$$

Where (X_j, Y_j) are the displacement vector of the journal center O_j in the fixed reference frame as shown in Figure 3.

(X_r, Y_r) are the absolute displacement components of the floating ring center O_r. $(\dot{X}_j, \dot{Y}_j)$ and $(\dot{X}_r, \dot{Y}_r)$ are the absolute velocities of O_j and O_r.

Therefore, the inner film eccentricity ε_i and outer film eccentricity □ε_o are as follows

$$\varepsilon_i = \frac{\sqrt{x_j^2 + y_j^2}}{c_i}, \quad \varepsilon_o = \frac{\sqrt{X_r^2 + Y_r^2}}{c_o} \tag{16}$$

Using Eqs. (10), (11),(12),(13) to substitute the oil film thicknesses and squeezed terms in above Eqs. (6), (7), they can also be expressed in the following format:

$$\frac{1}{\text{R}_j^2} \frac{\partial}{\partial \theta_i} \left[\frac{(c_i - x_j cos\theta_i - y_j sin\theta_i)^3}{12\eta_i} \frac{\partial p_i}{\partial \theta_i} \right] + \frac{\partial}{\partial z_i} \left[\frac{(c_i - x_j cos\theta_i - y_j sin\theta_i)^3}{12\eta_i} \frac{\partial p_i}{\partial z_i} \right] = \frac{\Omega_j + \Omega_r}{2} \frac{\partial (c_i - x_j cos\theta_i - y_j sin\theta_i)}{\partial \theta_i} - (\dot{x}_j cos\theta_i + \dot{y}_j sin\theta_i) \tag{17}$$

$$\frac{1}{\text{R}_{ro}^2} \frac{\partial}{\partial \theta_o} \left[\frac{(c_o - X_r cos\theta_o - Y_r sin\theta_o)^3}{12\eta_o} \frac{\partial p_o}{\partial \theta_o} \right] + \frac{\partial}{\partial z_o} \left[\frac{(c_o - X_r cos\theta_o - Y_r sin\theta_o)^3}{12\eta_o} \frac{\partial p_o}{\partial z_o} \right] = \frac{\Omega_r}{2} \frac{\partial (c_o - X_r cos\theta_o - Y_r sin\theta_o)}{\partial \theta_o} - (\dot{X}_r cos\theta_o + \dot{Y}_r sin\theta_o) \tag{18}$$

Eq. (17) and Eq. (18) turns out to be a partial differential equation, for which in general no analytic solution exists.

ISSN: 2230-9845 (Online), ISSN: 2321-516X (Print)

As a result, the associated domain, and by that the differential equation, has to be discretised in order to get a formulation, which is suitable for numerical solutions.

In [18, 19] the use of different methods is discussed such as FDM, FVM, FEM, BEM.

An essential point is the determination of the input quantities X_j, Y_j ,$\dot{X}_j$and $\dot{Y}_j$ that represent the direct link between the Reynolds equation Eq. (17), Eq. (18) the equation of motion Eq. (4).

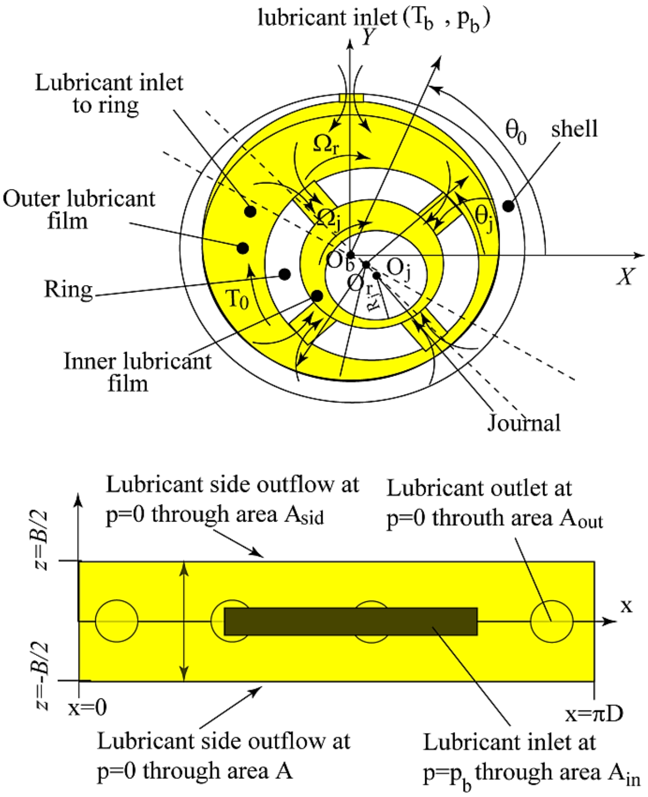

Figure 3. Scheme of typical hydrodynamic journal floating ring bearing.

Solving of equation of motion

Due to the high non-linearity of the MBD system, the equations have to be solved in the time domain. From equation (4) the kinematical quantities of rotor system can be obtained by using direct integral method.

In each time step, the equilibrium has to be fulfilled for both bodies and joints and the entire system.

In order to maximize numerical stability, direct implicit integration methods are used [21].

These methods inhibit velocities and accelerations at the new time step (ti+1 = ti + Δti), which are expressed by quantities at the time step ti and the state at ti+1

$$\dot{q}_{i+1} = \mu(\Delta t_i) q_{i+1} + \tau(\ddot{q}_i\,, \dot{q}_i\,, q_i\,, \Delta t_i) \tag{19}$$

$$\ddot{q}_{i+1} = \xi(\Delta t_i) q_{i+1} + \eta(\ddot{q}_i\,, \dot{q}_i\,, q_i\,, \Delta t_i) \tag{20}$$

The functions μ , τ , ξ and η are derived from a Taylor series expansion for q_{i+1} , $\dot{q}_{i+1}$, and can be expressed by

$$\tau = -\frac{\gamma}{\beta \Delta t_i} q_i - \left(\frac{\gamma}{\beta} - 1\right) \dot{q}_i - \frac{\Delta t_i}{2} \left(\frac{\gamma}{\beta} - 2\right) \ddot{q}_i \tag{21}$$

$$\mu = \frac{\gamma}{\beta \Delta t_i} \tag{22}$$

$$\eta = -\frac{1}{\beta \Delta t_i{}^2}\, q_i - \frac{1}{\beta \Delta t_i}\, \dot{q}_i - \left(\frac{1}{2\beta} - 1\right) \ddot{q}_i \tag{23}$$

$$\xi = \frac{1}{\beta \Delta t_i{}^2} \tag{24}$$

Where γ is Newmark parameter for dissipation control, β is Newmark parameter for acceleration control.

Applying the solution q_{i+1} at time t_{i+1} in addition to (19) and (20) to the system equation of motion(4) yields a linear equation system [22,23]

$$\bar{K} q_{i+1} = \bar{F}_{i+1} \tag{25}$$

with the effective stiffness matrix

$$\bar{K} = \frac{1}{\beta \Delta t_i{}^2} M + \frac{\gamma}{\beta \Delta t_i} D + K \tag{26}$$

and the effective vector of forces and moments

$$\bar{F} = F_{i+1}^{a} + F_{i+1}^{oil} + M\left(\frac{1}{\beta \Delta t_i{}^2} q_i + \frac{1}{\beta \Delta t_i} \dot{q}_i + \left(\frac{1}{2\beta} - 1\right) \ddot{q}_i\right) + D\left(\frac{\gamma}{\beta \Delta t_i} q_i + \left(\frac{\gamma}{\beta} - 1\right) \dot{q}_i + \Delta t_i \left(\frac{\gamma}{2\beta} - 2\right) \ddot{q}_i\right) \tag{27}$$

Equation (25) is solved by standard methods.

To solve the equation (25), the oil film force must be found in each time steps of the force vector.

At first, the appropriate must be given from the previous time step to get.

By using this value, we can obtain in equation (25).

From equation (17) and (18) we can get oil film force by using.

This calculation is repeated until the calculated force and displacement is in error limit.

Error calculation is as follows:

$$\frac{\sum_{k=1}^{n} \left| F_{k,i+1}^{a\ j+1} - F_{k,i+1}^{a\ j+1} \right|}{\sum_{k=1}^{n} max\left(\left| F_{k,i+1}^{a\ j+1} \right|, \left| F_{k,i+1}^{a\ j} \right| \right)} < \varepsilon(F^{a}) \tag{28}$$

$$\frac{\sum_{k=1}^{n} \left| F_{k,i+1}^{oil\ j+1} - F_{k,i+1}^{oil\ j+1} \right|}{\sum_{k=1}^{n} max\left(\left| F_{k,i+1}^{oil\ j+1} \right|, \left| F_{k,i+1}^{oil\ j} \right| \right)} < \varepsilon(F^{oil}) \tag{29}$$

$$\frac{\sum_{k=1}^{n} \left| q_{k,i+1}^{j+1} - q_{k,i+1}^{j+1} \right|}{\sum_{k=1}^{n} max\left(\left| q_{k,i+1}^{j+1} \right|, \left| q_{k,i+1}^{j} \right| \right)} < \varepsilon(\mathrm{q}) \tag{30}$$

RESULTS AND ANALYSIS

In this section, the main working characteristics are considered in several ratios.

Figure 4 shows the track of the journal and floating ring at rotating speed of 110000rpm.

This speed was chosen as working speed of turbocharger.

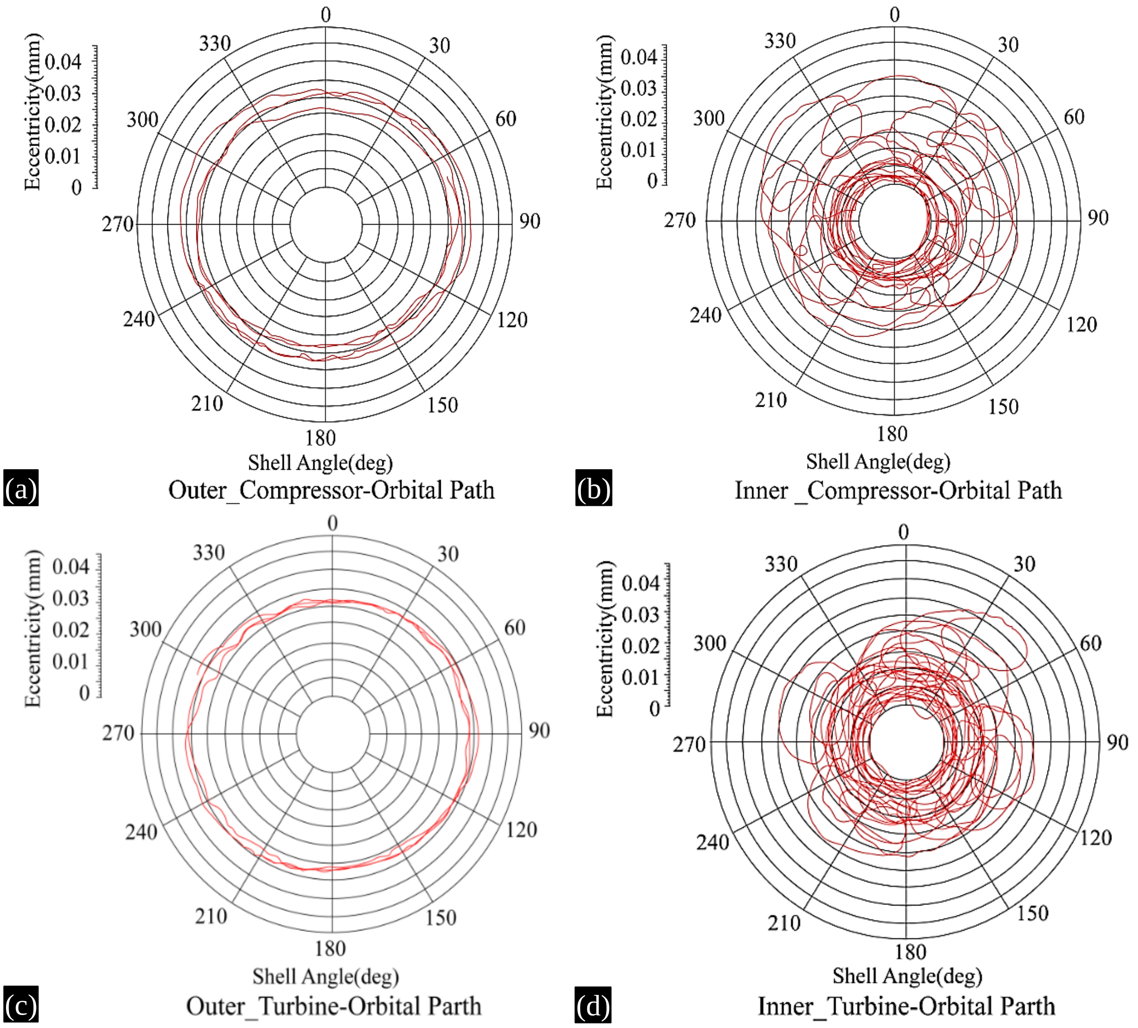

Figure 4. (a-d) The track of the journal and floating ring at rotating speed of 110000rpm.

Figure 5 shows the main working condition of outer oilfilm of compressor floating ring bearing when $D_0/D_i = 1.52,\ L_0/L_i = 1.4, C_o/C_i = 2.19$.

Figure 6 shows the oil mass flow of outer oilfilm, friction loss and the thickness of minimum oilfilm according to the variety of diameter ratio, length ratio and clearance ratio [24].

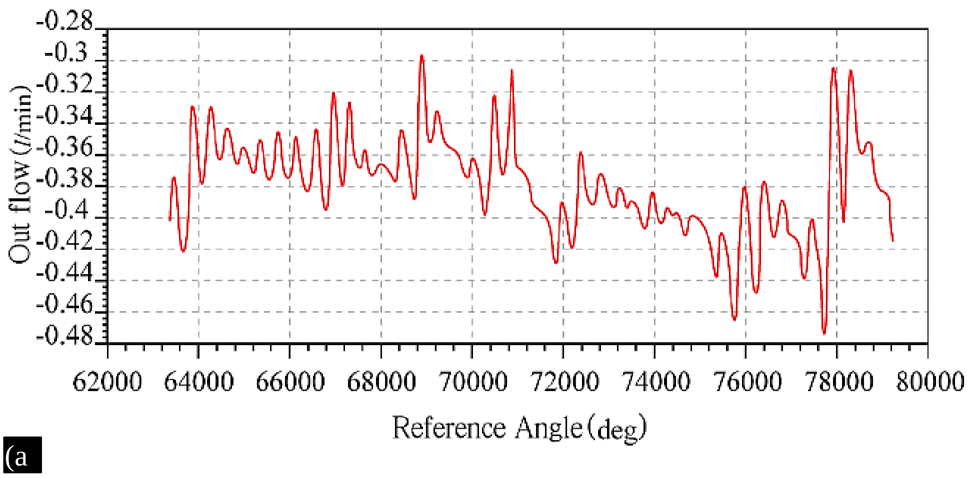

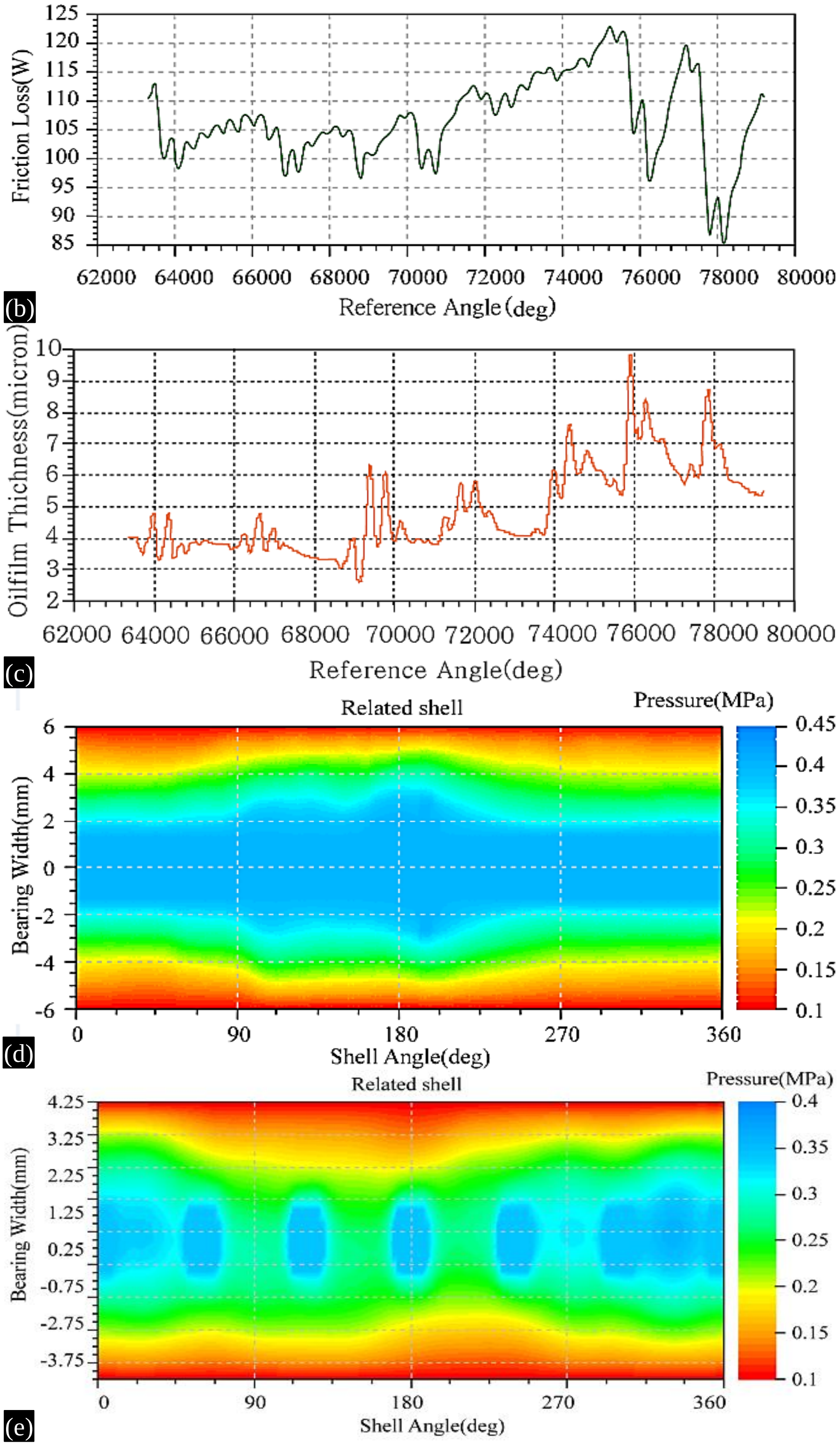

Figure 5. The main working condition of oilfilm of FRB at the point of compressor when the diameter ratio is 1.52, (a) Oil flow out of bearing, (b) Friction loss, (c) Minimum oilfilm thinkness, (d) Total average pressure of outer oilfilm, (e) Total average pressure of inner oilfilm.

Journal of Experimental & Applied Mechanics
Volume 15, Issue 3
ISSN: 2230-9845 (Online), ISSN: 2321-516X (Print)

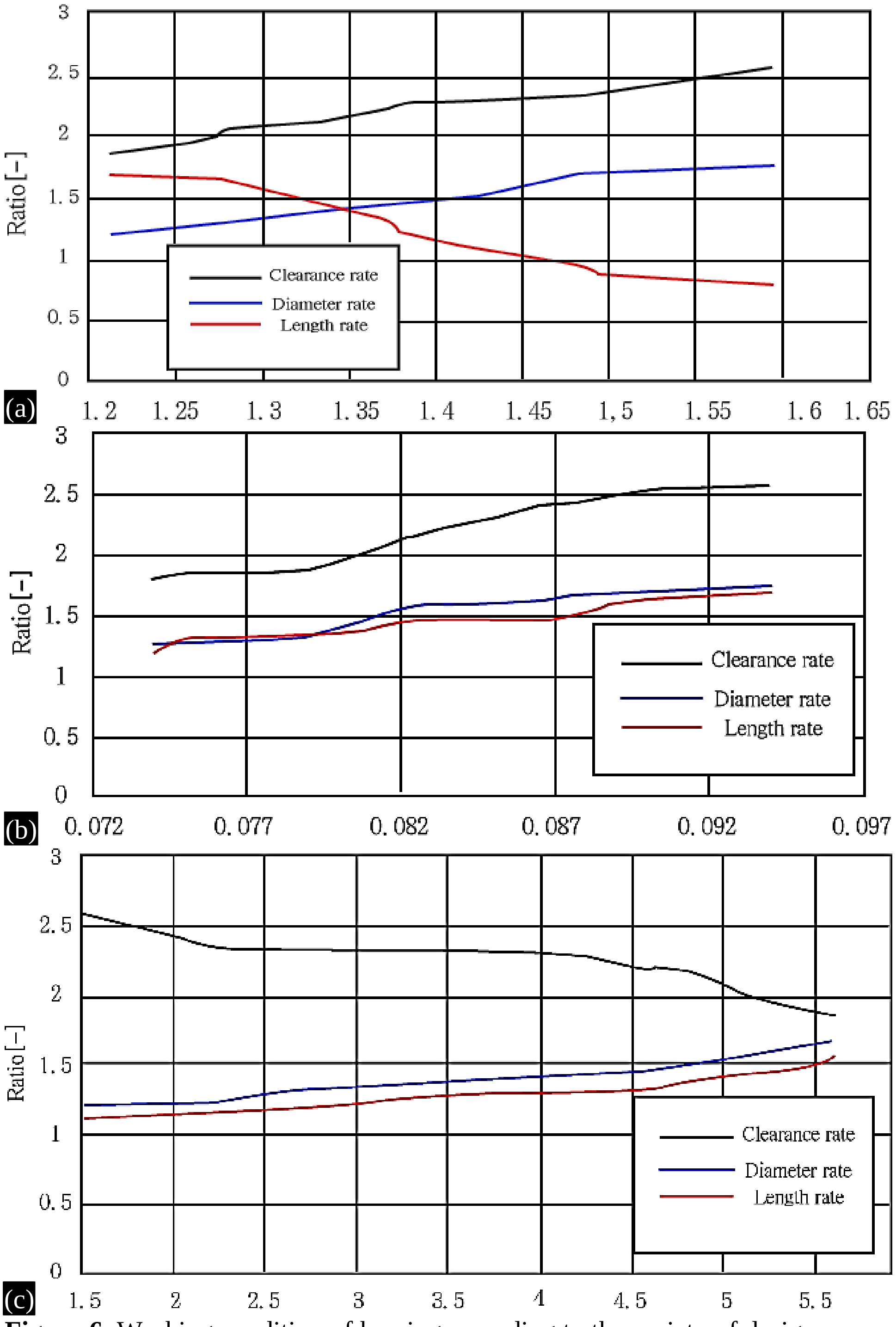

Figure 6. Working condition of bearing according to the variety of design parameters of floating ring bearing, (a) Cubic flow rate, (b) Frictional loss, (c) Thickness of minimum oilfilm

The influence of diameter ratio to the main working characteristics of FRBs

As you can see in Figure 6, the total friction loss is increased as the diameter ratio is increased.

Also, the oil mass flow in FRBs gets more.

The higher the diameter ratio, the more the minimum thickness of outer oilfilm.

This is because the stiffness coefficient is increased and the movement to the outer oilfilm is more difficult.

The bearing damage can be occurred in the field between the shaft and inner bearing when the diameter ratio is too high.

The range of diameter ratio is limited in finite field at the given of the shaft diameter and the outer diameter of shell(turbocharger body).

In real turbocharger the diameter ratio is chosen as 1.52 because the high diameter ratio is good at the point of view of the rotor stability but too high value is not good as the point of view of the main working quantities.

It is also limited in the geometrical size and it has the advantages and disadvantages, so it is chosen on the basis of calculation data [20-24].

The influence of the length ratio on the working characteristics of FRBs

From Figure 6 you can know the oil mass flow condition of outer oilfilm of compressor FRB on the variety of length ratio.

As you can see in the figure, the oil mass flow passing the FRB decreases when the length ratio increases.

This is described as the increase friction force on the FRB surface.

This increase of friction force causes the improvement of rotor stabilization and the decrease of rotor amplitude in resonance.

As you know, the minimum thickness of outer oilfilm increases when the length ratio increases.

This is described as the increase of stiffness coefficient of outer oilfilm, so the movement of the bearing ring to the outer oilfilm gets more difficult.

So the bearing damage can be occurred between the shaft and inner bearing.

So we must pay attention to the choosing of length ratio. From [5,6,8], it is good to choose that value from 1.2 to 1.6.

The influence of clearance ratio to the main working characteristics fo FRBs

Figure 6 shows the fluid dynamical friction loss in the outer oilfilm gap.

At the given conditions, the friction loss gets larger according to the increase of clearance ratio.

This is because the loss gets bigger according to the increase of the clearance.

Figure 6. the working state of outer oilfilm

The large clearance ratio improves the rotor stabilization and causes the noise in air in resonance.

The larger the clearance ratio, the more the oil mass flow passing the FRB.

The thickness of minimum oilfilm thickness gets smaller.

This is the decrease of the stiffness coefficient of outer oilfilm, so it makes the movement of the bearing ring to the outer oilfilm easy and can reduce the damage between the shaft and the inner bearing.

Too high outer bearing clearance can cause the high rotor error in the outer oilfilm.

This analysis corresponds to the numerical results introduced in [4, 10,24].

CONCLUSION

The design parameters of FRBs such as length ratio, diameter ratio are affected to the working characteristics. So they must be chosen seriously.

As you can see in the result and analysis, the most important factor is the clearance ratio in them.

The field of the thickness of minimum oilfilm contains from 1.87 to 2.57 and it is more affected to the working characteristics than any others.

Also, it is the most convenient to change the clearance as a design parameter.

The clearance ratio must be big enough to have the inherent characteristics of FRBs.

The clearance ratio is limited by the inner oilfilm gap.

The outer oilfilm must be decided by the minimum oilfilm thickness due to the loss of oil mass flow in outer oilfilm and the loss of stiffness coefficient.

The inner oilfilm gap is mainly related to temperature raise of oil by the fluid dynamical friction.

Besides that, some parameters such as oil form, oil input temperature, pressure, rotor velocity range and valence must be considered in various working conditions.

REFERENCES

1. H. Ma, Z. Wu, X. Tai, B. Wen, Dynamic characteristics analysis of a rotor system with two types of limiters. International Journal of Mechanical Sciences 88 192-201, 2014. (8,5)
2. C. Gan, Y.Wang, S. Yang, Y. Cao, Nonparametric modeling and vibration analysis of uncertain Jeffcott rotor with disc offset. International Journal of Mechanical Sciences 78 126134, 2014. (8,3)
3. LI C H, ROHDE S M, On the steady state and dynamic performance characteristics of floating ring bearings[J]. Journal of Lubrication Technology-Transactions of the ASME, 1981, 103: 389–397. (5)
4. Hung Nguyen-Schäfer H, Rotordynamics of Automotive Turbochargers. Springer, 2012.
5. WANG Longkai, BIN Guangfu, Effects of Floating Ring Bearing Manufacturing Tolerance Clearances on the Dynamic Characteristics for Turbocharger. Chinese Journal of Mechanical Engineering, 2015, 28(3): 530–539.
6. TIAN L, WANG W J, PENG Z J, Effects of bearing outer clearance on the dynamic behaviors of the full floating ring bearing supported turbocharger rotor[J]. Mechanical Systems and Signal Processing, 2012, 31(0): 155–175.
7. C.A. Papadopoulos, P.G. Nikolakopoulos and G.D. Gounaris, Identification of clearances and stability analysis for a rotor-journal bearing system. Mechanism and Machine Theory, 43, 411-426,2008. (8,14)
8. Luboš Smolik, Michal Hajžman, Miroslav Byrtus, Investigation of bearing clearance effects in dynamics of turbochargers. International Journal of Mechanical Sciences,DOI: 10.1016/j.ijmecsci.2016.07.013.
9. B. Schweizer, M. Sievert, Nonlinear oscillations of automotive turbocharger turbines, Journal of Sound and Vibration 321 (3- 5) (2009) 955–975. doi:10.1016/j.jsv.2008.10.013. (16,37)
10. Schweizer B , Rieger NF , Black HF , Thomas ChB . Dynamics and stability of turbocharger rotors. Arch Appl Mech 2010;80(9) ISSN 0939-1533 (17,4) .
11. Dakel M, Baguet S, Dufour R, Nonlinear dynamics of a support-excited flexible rotor with hydrodynamic journal bearings[J]. Journal of Sound and Vibration, 2014, 333(10): 2774–2799. (5,10)

12. TIAN L, WANG W J, PENG Z J, Dynamic behaviors of a full floating ring bearing supported turbocharger rotor with engine excitation[J]. Journal of Sound and Vibration, 2011, 330(20): 4851–4874. (5,14)
13. SHI Wei, WEI Daogao, ZHU Lei, et al, Study on effects of clearance ratio of inner to outer film on turbocharger rotor instability[J]. Chinese Journal of Automotive Engineering, 2014,4(2): 130–136. (in Chinese). (5,16)
14. GUNTER E J, CHEN W J, Dynamic stability and whirl motion of large diesel engine turbochargers in floating bush and multi-lobed bearings[C]//Vibration Institute 34th Annual Meeting, Illinois, USA,June 22–26, 2010. (5,20)
15. CHEN W J, GUNTER E J, Introduction to dynamics of rotor-bearing systems[M]. Victoria: Trafford Publishing, 2010. (5,23)
16. E. Woschke, C. Daniel, S. Nitzschke, Excitation mechanisms of non- linear rotor systems with floating ring bearings - simulation and validation, International Journal of Mechanical Sciences (2017), doi:10.1016/j.ijmecsci.2017.09.038.
17. Pavel Novotný, Petr Š kara, Juraj Hliník, The effective computational model of the hydrodynamics journal floating ring bearing for simulations of long transient regimes of turbocharger rotor dynamics. International Journal of Mechanical Sciences.148(2018) 611-619.
18. L. R. Gero, C. M. McC.Ettles, An evaluation of finite difference and finite element methods for the solution of the reynolds equation, ASLE Transactions 29 (1986) 166–172. doi: 10.1080/05698198608981674. (16,22)
19. Q. Yu, T. G. Keith Jr, A boundary element cavitation algorithm, Tribology transactions 37 (2) (1994) 217–226. doi:10.1080/10402009408983286. (16,23)
20. Y. Hori, Hydrodynamic Lubrication. Springer, Tokyo, 2006. (16,33)
21. G. W. Stachowiak and A. W. Batchelor, Engineering Tribology. 4th Ed.St. Louis: Butterworth-Heinemann, 2014. (8,31)
22. Homer Rahnejat,Tribology and dynamics of engine and powertrain, Woodhead Publishing,2010.
23. AVL List Gmbh, Theory AVL EXCITE POWER UNIT VERSION 2013.2, Oct. 30, 2013.
24. P. A. Lakshminarayanan, Avinash Kumar Agarwal, Design and Development of Heavy Duty Diesel Engines, Springer, 2020.

